Distribution and Influence of Iron Phases on the Physico-Chemical Properties of Phyllosilicates

MERVAT SAID HASSAN
(*Central Metallurgical R and D Institute, Cairo, Egypt*)
SAYED MAHMOUD SALEM
(*Physics Department, Faculty of Science, Al-Azhar University, Naser City, Cairo, Egypt*)

Abstract: Clay minerals from different Cretaceous stratigraphic successions of Egypt were investigated using XRD, DTA, dissolution analysis (DCB), IR, Mössbauer and X-ray Electron Spin Resonance (ESR) spectroscopes. The purity of the samples and the degree of their structural order were determined by XRD. The location of Fe in the octahedral sheet is characterized by absorption bands at $\sim 875 cm^{-1}$ assigned as Al-OH-Fe which persist after chemical dissolution of free iron. The Mössbauer spectra of these clays show two doublets with isomer shift and quadrupole splitting typical of octahedrally coordinated Fe^{3+}, in addition to third doublet with hyperfine parameter typical of Fe^{2+} in the spectra of Abu-Had kaolinite (H) sample. Six-lines magnetic hyperfine components which are consistent with those of hematite are confirmed in the spectra of both Isel and Rish kaolinite samples. Goethite was confirmed by both IR and DTA. Multiple nature of ESR of these clays suggested structural Fe in distorted octahedral symmetry as well as non-structural Fe.

Little dispersion and low swelling indices as well as incomplete activation of the investigated montmorillonite samples by $NaCO_3$ appear to be due to incomplete disaggregation of montmorillonite particles. This can be explained by the ability of Fe-gel to aggregate the montmorillonite into pseudo-particles and retard the rigid-gel structure. However, extraction of this ferric amorphous compound by dithonite treatment recovers the surface properties of the montmorillonite samples.

On the other hand, the amount and site occupation of Fe associated with kaolinite samples show an inverse correlation with the parameters used to describe the degree of crystallinity perfection, color, brightness and vitrification range of these kaolinite samples.

Key words: **Cretaceous clay; iron phase; mineralogy; DCB treatment; spectroscopy; dispersion; crystallinity index**

Introduction

Iron in clays and clay minerals influences their commercially important characteristics such as color, brightness, hydraulic conductivity, ion exchange capacity and other colloidal rheological and chemical properties. Not only is the amount of iron important, but also the oxidation state plays a critical role in determining the commercial value of a clay and whether or not beneficiation will be effective. Recently, spectroscopy (e.g. Mössbauer, electron spin resonance and infrared spectroscopy) has become an important tool in research on clay minerals. A number of clay minerals including montmorillonite, kaolinite, illite and mica have been studied with regard to their p-

ISSN 1000-9426

aramagnetic species either within the aluminosilicate structure or as an external impurity phase (Mendelovici et al., 1979; Coey, 1980; Heller-Kallai and Rozenson, 1981; Bahranowski et al., 1993). The present investigation was undertaken to find out by selective chemical dissolution the distribution of Fe in the clay minerals from different Cretaceous stratigraphic successions of Egypt using IR, DTA, Mössbauer spectroscopy and electron spin resonance, as well as relationship between the nature and amount of iron and the other parameters of clay minerals, especially disaggregation and rheological properties of montmorillonite and the degree of crystal perfection in kaolinite, brightness and vitrification range of kaolinite samples.

Materials and technique

Six samples were examined in the present study. Details of their mineralogical and chemical composition are given in Tables 1 and 2. They were classified as two groups: 1) the first group (SH_1 and SH_9) in which Ca-montmorillonite is the main component in addition to kaolinite; and 2) the second group (Wadi-Qisieb K, Wadi Abu-Had-H, Iseila-Isel and Abu-ElReesh-Rish) in which kaolinite mineral was the main component in addition to traces of illite, montmorillonite and quartz. The kaolinite sample varies in iron content and crystallinity (Table 3). Rheological properties as well as swelling indices of natural and deferrated montmorillonite were measured according to the standard procedures of the American Petroleum Institute. The purity of the samples and the degree of structural order were determined with XRD using Philips PW1730 with Ni filtered and Cu-radiation as well as differential thermal analyses (DTA).

Table 1. Mineralogical composition of the investigated samples

Sample No.	Origin	XRD impurities
SH_1	Nile Valley (Up. Cretaceous)	Kaolinite and quartz
SH_9	Nile Valley (Up. Cretaceous)	Kaolinite and quartz
Wadi-Qisieb (K)	Red Sea (L. Cretaceous) 90km S. Suez	Quartz and illite
Abu-Had (H)	Red Sea (L. Cretaceous) 80km, W. of Ras Gharib.	Quartz and feldspar
El-Iseila (Isel)	NE Abu-Zenima (L. Cretaceous)	Quartz, illite and hematite
Abu El-Reesh (Rish)	Aswan (Cretaceous)	Quartz, illite and hematite

Table 2. Chemical composition of the investigated samples

Sample No.	SiO_2	Al_2O_3	Fe_2O_3	TiO_2	MgO	CaO	Na_2O	K_2O	L.O.I
SH_1	61.81	14.78	4.74	0.5	1.93	0.8	1.93	0.83	12.68
SH_9	65.09	15.81	4.05	0.83	1.61	0.65	1.61	0.86	9.39
Wadi-Qiesib (K)	62.30	29.42	0.5	0.6	0.13	0.13	0.03	0.46	8.85
Abu-Had (H)	73.9	17.52	0.62	1.27	0.12	0.11	0.03	0.47	6.3
El-Iseila (Isel)	49.46	35.73	1.7	3.53	0.15	0.17	0.04	0.23	12.50
Abu El-Reesh (Rish)	56.22	23.23	5.98	1.83	0.5	0.59	0.2	0.48	9.07

Selective chemical dissolution

Extraction of free iron by ditonite-citrate bicarbonate (DCB) was carried out according to Mehra and Jackson (1960). 250 mg of the investigated samples were deferrated with DCB at 75℃ in stirred water bath. After 30 min the supernatant was separated and analyzed for iron. The process was repeated several times (3 – 8), depending on iron content, until the DCB extraction solution was free of iron.

Infrared spectroscopy

IR absorption spectra were recorded from 4000 − 220 cm^{-1} for original and deferrated samples from Kbr disks with Jasco 5200 spectrometer.

Mössbauer spectroscopy

Mössbauer measurements were performed by the constant acceleration method at room temperature, with a source of cobalt-57 (20 mCi) diffused into a Rh matrix. The velocity of the spectrometer was calibrated using an iron metal absorber, which was also used as a reference for the isomer shift value.

Electron spin resonance

ESR measurements were carried out on a Varian spectrometer (model E3). The g values were measured with a DPPH standard ($g = 2.0036$). The sample tubes were usually filled with clay powder to a height greater than that of the cavity. All the experiments were carried out at room temperature.

Results and Discussion

Deferrated clays

All dithonite treatment of the raw materials produces whitish-grey to grey residues. It is evident that the materials producing the red or yellow colors are present in the free Fe oxide fractions. The total concentrations of free iron-oxide and structural iron in alumino-silicate minerals are indicated by the difference between total Fe and dithonite Fe in Table 3. According to Childs and Goodman (1987), hematite and goethite may be present in red clay minerals but hematite is always absent from yellow one. We were aware that the failure to have detected hematite and goethite in the majority of the studied samples may be due to the poor sensitivity of XRD to Fe-oxide and oxyhydroxide present at low levels and in small particle-size. However, the presence of goethite has been confirmed by means of DTA of some samples, especially montmorillonite samples as poorly crystalline phase.

Table 3. Iron contents and crystallinity indices for the investigated samples

Sample No.	Colour	Total Fe (wt%)	Dithonite Fe (wt%)	H.I.
SH_1	Yellow	4.47	1.2	–
SH_9	Yellow	4.05	0.7	–
Wadi-Qiesib (K)	Grey	0.5	0.05	1.5
Abu-Had (H)	Grey	0.6	0.09	0.49
El-Iseila (Isel)	Pink	1.70	0.75	0.79
Abu El-Reesh (Rish)	Buffe	5.98	1.94	0.43

Infrared spectroscopy

The effect of deferration process on the IR spectra of investigated samples can be clearly seen in Figs. 1 and 2, where the broad distorted bands of the untreated samples become narrower and show greatly improved resolution. On the other hand, the absorption band at 800 cm^{-1} which oc-

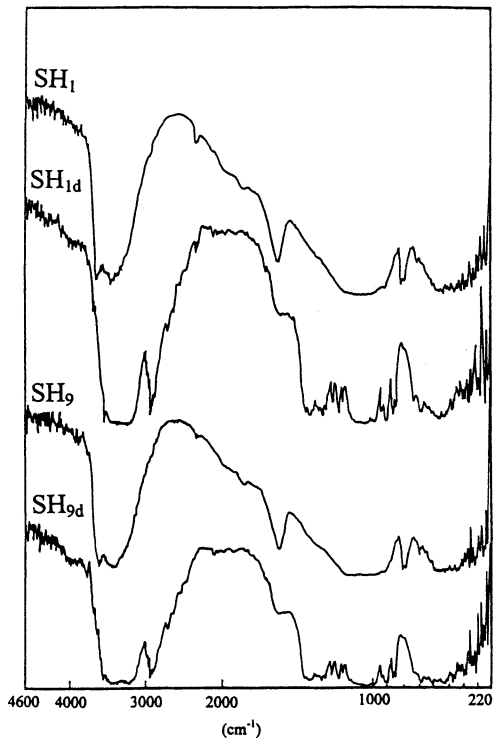

Fig. 1. Infrared spectra of montmorillonite samples. SH_1, SH_9 = Original samples; SH_{1d}, SH_{9d} = deferrated samples.

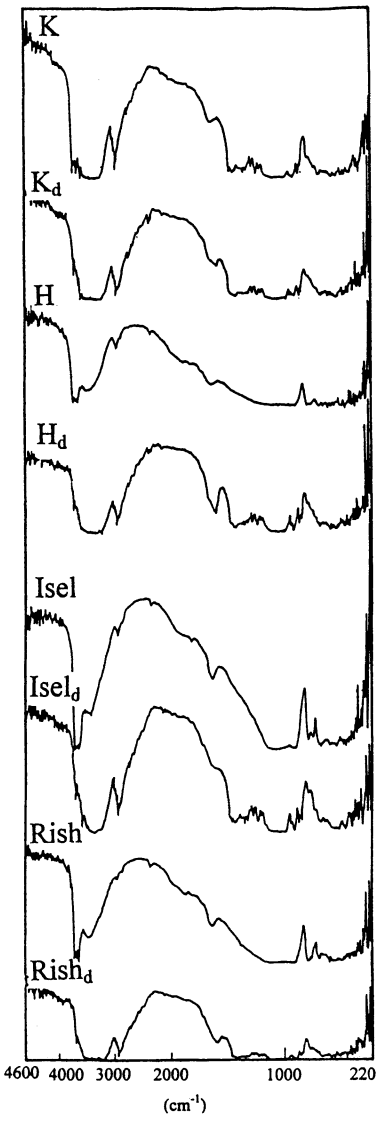

Fig. 2. Infrared spectra of kaolinite samples. K, H, Isel, Rish = Original samples; K_d, H_d, $Isel_d$, $Rish_d$ = deferrated samples.

curs between clay minerals (montmorillonite and kaolinite) and goethite becomes less intense after deferration process. The relative shift in peak position of OH deformation band of Al-Fe-OH group to 870 cm^{-1} in the spectra of montmorillonite samples (Fig. 1) is being diagnostic of increasing substitution of Al by Fe in structural lattice. According to Goodman et al. (1976), the position of the absorption maximum of the Al-Fe-OH varies with the group of smectite. It shifts to 847 − 1 in Garfield nontronite (Stuki and Roth, 1976), to 851 cm^{-1} in Nova ves nontronite (Grman et al., 1973), to 880 cm^{-1} in Woburn Fullers Earth (Heller et al., 1962) and to 889 cm^{-1} in Wyoming montmorillonite (Farmer et al., 1967). From this it would appear that the Al-Fe-OH vibration occurs at higher frequency when the neighboring cations are aluminum whereas it has lower frequency when they are iron. Moreover, the weak to moderate high-frequency band at 875 cm^{-1} arises from small amounts of iron in kaolinite mineral, producing the grouping of Al-Fe-OH (Fig. 2). Mendelovici et al. (1979) concluded that thermal treatment of kaolinite has no effect on the intensity of the 875 cm^{-1} band and the latter persists up to 420℃. It begins to disappear at 420℃ when the kaolinite starts to decompose thermally.

Mössbauer spectroscopy

The room-temperature Mössbauer spectra of the SH_1 and SH_9 samples (Fig. 3) are satisfactorily analyzed as a superposition of two quadrupole doublets with different isomer shifts (δ) and quadruple splitting (Q). Data for the fitting procedure for this study are presented in Table 4. The hyperfine parameters for these doublets indicate that they can all be assigned to ferric iron in octahedral coordination. The two $^{Vi}Fe^{3+}$ doublets have isomer shift and quadrupole splitting values of approximately 0.37, 0.4 mm/s (A) and 0.37 − 0.76 mm/s (B), respectively. Such values are consistent with those of Rozenson and Heller-Kallai (1977). The A doublet with hyperfine parameters of $\delta = 0.36$ mm/s and $Q = 0.39$ mm/s at Rt, is assigned to ferric iron in cis-octahedral coordination and it is corresponding to 70% of the total peak area. The isomer shift value of 0.36 mm/s for doublet B indicates that Fe^{3+} is in octahedral coordination. However, it is not clear, based on quadrupole splitting values, the Fe^{3+} has cis or trans octahedral occupance. According to Buatier et al. (1993), the value of 0.76 mm/s for the quadrupole splitting can be explained by the coordination of Fe atom. A3R3 configuration, i.e., octahedral Fe^{3+} neighbors, explains the value of 0.76 mm/s.

As the best fit of the spectra implies Fe only in octahedral sites, the result of this Mössbauer study is the absence of tetrahedral Fe in all the studied samples. However, the occurrence of iron oxide was not demonstrated from Mössbauer analysis at RT. It is confirmed by IR, DTA and chemical dissolution. The presence of iron oxyhydroxide (goethite) was confirmed by IR and DTA. The DCB treatment was used to remove iron oxyhydroxide present in interlayers or as staining. As shown in Fig. 4, the Mössbauer spectra of deferrated samples are very similar to those of original samples. Meanwhile, the quantitative analysis of the spectra after dithonite treatment indicates that the intensities of the doublet due to Fe^{3+} (A) were reduced. The latter reveals the superposition of a doublet due to super-paramagnetic iron-oxyhydroxide with that of Fe^{3+} substituted in the cis-site of octahedral lattice (Fig. 4).

Table 4. Mössbauer parameters and abundance of the raw samples at RT

Sample No.	Fe^{3+} (cis)			Fe^{3+} (trans)			Fe^{2+}		
	δ(mm/s)	Q(mm/s)	%	δ(mm/s)	Q(mm/s)	%	δ(mm/s)	Q(mm/s)	%
SH_1	0.364	0.376	71.43	0.371	0.761	28.57	–	–	–
SH_9	0.353	0.41	60.50	0.346	0.74	39.50	–	–	–
K	0.349	0.471	31.70	0.362	0.96	68.60	–	–	–
H	0.27	0.77	23.30	0.367	1.06	37.80	1.37	2.53	38.50
Isel	0.31	0.52	20.33	0.34	0.97	60.00	–	–	–
Rish	0.31	0.476	11.27	0.32	0.815	21.55	–	–	–

On the other hand, all the spectra of kaolinite samples (Fig. 3) were computer fitted to yield the best values of the hyperfine parameters. These parameters show that, in all the spectra the iron occurs only in ferric state except (H) sample which contains iron in both Fe^{3+} and Fe^{2+} states. This fraction of Fe^{2+} in (H) sample may decrease the symmetry of the sample and cause octahedral site distortion to increase possibly due to the fact that Fe^{2+} is significantly larger than both Al^{3+} and Fe^{3+} (Murad, 1994). That also appears in the larger isomer shift (1.37 mm/s) and quadrupole splitting (2.5 mm/s) of Fe^{2+} than that of Fe^{3+}. The previous result is confirmed by the crystalline index of (H) sample (Table 3). The Mössbauer spectra of Isel and Rish (Fig. 3) showed 6-lines magnetic hyperfine components, which are consistent with those of hematite. According to Childs and Goodman (1987) neither akaganeite nor lepidocrocite have 6-lines spectra

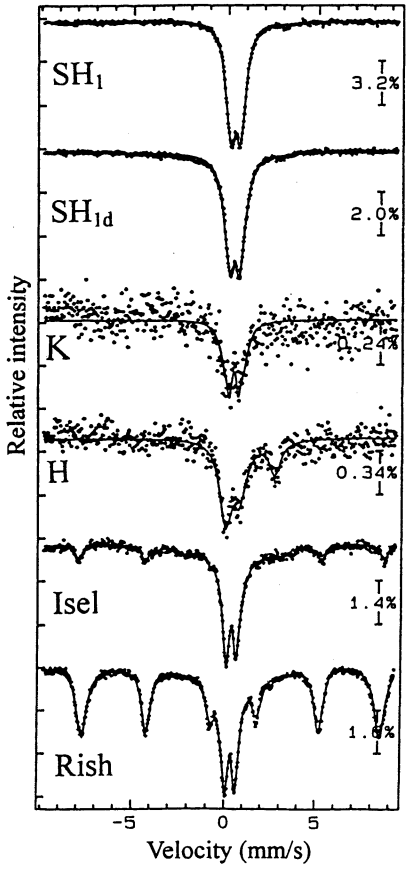

Fig. 3. Mössbauer spectroscopy of original montmorillonite and kaolinite samples. The symbols are the same as in Figs. 1 and 2.

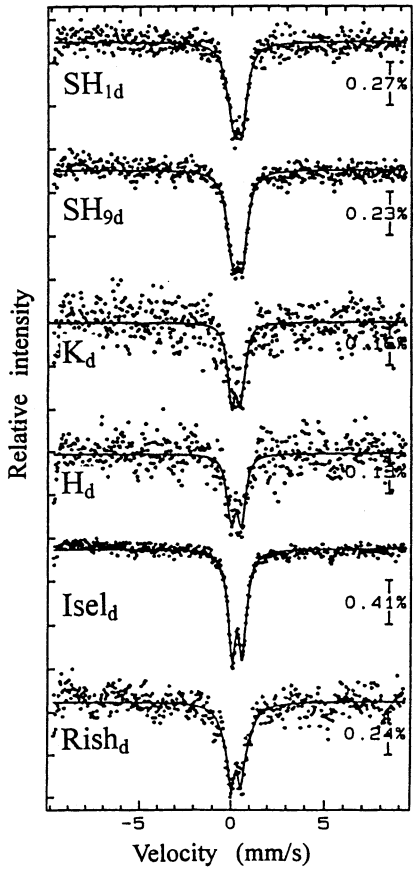

Fig. 4. Mössbauer spectroscopy of deferrated montmorillonite and kaolinite samples. The symbols are the same as in Figs. 1 and 2.

at room temperature. Meanwhile, after dithonite treatment the spectra of these two samples (Fig. 4) showed the disappearance of the 6-lines magnetic hyperfine components indicating the removal of free Fe-oxide. The quantitative analysis of the spectra after dithonite treatment indicates that the intensities of the doublet due to Fe_3 in cis-site were reduced. The latter reveals the superposition of a doublet due to super-paramagnetic iron-oxide with that of Fe^{3+} substituted in the cis-site of octahedral lattice (Fig. 4).

Electron spin resonance

The ESR of the untreated montmorillonite samples is shown in Fig. 5. The multiple nature of the resonance with g-values approximately equal to 2.0, 2.2, 3.7, 4.3, and 9.6 shows a qualitative similarity to the spectra of Goodman (1978). The features with ~3.7, 4.3 and 9.6 can be interpreted as arising from Fe^{3+} in sites of near rhombic symmetry. The broad feature with $g \approx 2$ must arise from Fe^{3+} in a different type of environment. The weak narrow feature with $g = 2.0$ probably arises from an unpaired electron at a surface or bulk defect site. The weak resonance at $g \approx 3.7$ has been interpreted in connection with octahedral Mg^{2+} ion in montmorillonite (McBride et al., 1975). Meanwhile, the ESR of the untreated kaolinite samples is shown in Figs. 6-7. In general there are two principal resonances at $g = 2.0$ and $g = 4.2$. The line shape

and intensity of both resonances vary. At g = 4.2, the intensity of the central line decreases in the order of Rish > Isel > H > K while the intensity of the addition lines on both sides of the central line decreases in the reverse order. The latter resonance (g = 4.2) which is present in all the investigated samples is associated with the distorted octahedral symmetry (Mestdagh et al., 1980; Shakium and Carr, 1987 and Bahranowski et al., 1993). There is a correlation between the lineshape of the g = 4 signal and the crystalline order of the kaolinite samples. The intensity of this signal is inversely proportional to the degree of crystallinity for kaolinite. For instance, when going from Rish sample with low crystallinity (Table 3) to well crystalline kaolinite (K), the g = 4 band decreases in intensity and gains more pronounced shoulders, while the g = 2 sharp doublet increases in intensity. From the spectra (Figs. 6 - 7) it may be seen that all the samples excluding (K) and (H) samples contain non-structural forms of iron which produced more or less pronounced broad signal at g = 2. The broadening of this signal increases as the non-structural iron increases in the order of Rish > Isel > H > K. Both chemical and Mössbauer analyses revealed that Rish and Isel samples have the largest amounts of total and structural iron, respectively.

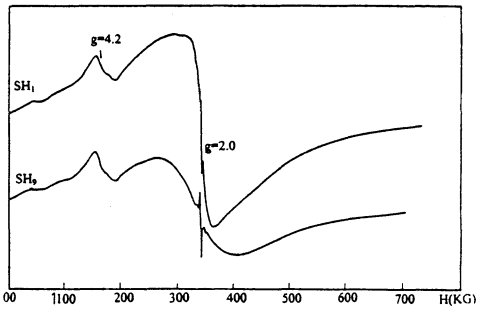

Fig. 5. ESR of original montmorillonite samples. The symbols are the same as in Fig. 1.

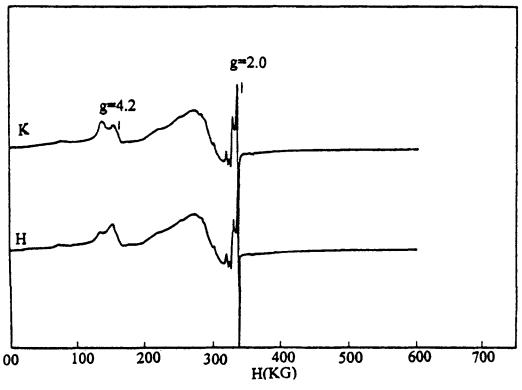

Fig. 6. ESR of original kaolinite samples (K and H). The symbols are the same as in Fig. 2.

Dispersion state of montmorillonite in water before and after DCB

Without pretreatment, dispersion or swelling indices of the studied montmorillonite samples (Table 6) are very low even when the pH is increased by the addition of $NaCO_3$, showing that montmorillonite particles interaction is not dependent only on electrostatic bonds between surface areas whose charge could be modified by pH, but there is a strong bond between particles, which is broken only after DCB treatment. The responsible agent of this chemical bond is the weakly crystallized Fe-oxyhydroxide (goethite) present in small amounts and in amorphous state (undetected by XRD, such as Fe-form soluble in DCB). According to Kinniburg et al. (1975), the weakly crystallized Fe-oxide with an isoelectric point > 8.1 has reduced the zero point of charge of the iron-clay association. This hypothesis accords with many studies whose emphasis is placed on the aggregation role of these amorphous ferric compounds (Blackmore, 1973; Robert et al., 1981; Michalete et al., 1993) as opposite to well crystallized oxide. This conclusion is very similar to that of Pedro et al. (1976) who dispersed clays which were aggregated into pseudo-particles of oxisols after an oxalate treatment. These pseudo-particles could form morphological units with very different surface properties and behaviours (CEC, swelling capacity, etc.) from those of free clays.

Extraction of these ferric compounds "deferrated clay" recovers surface properties and facilitates the alkali activation of the investigated samples, consequently improving the rheological properties (Table 6). Also, by the effect of this treatment (DCB), we think that we have shown the essential principle of the dispersion and, in this way, of the behavior of "clay-ferric oxyhydroxide-amorphous" associations.

Table 5. Mössbauer parameters and abundance of the samples after dithonite treatment at RT

Sample No.	Fe^{3+} (cis)			Fe^{3+} (trans)			Fe^{2+}		
	δ(mm/s)	Q(mm/s)	%	δ(mm/s)	Q(mm/s)	%	δ(mm/s)	Q(mm/s)	%
SH_{1d}	0.364	0.376	23.99	0.371	0.761	76.01	–	–	–
SH_{9d}	0.353	0.41	20.83	0.346	0.74	79.17	–	–	–
K_d	0.349	0.471	1.70	0.362	0.96	98.23	–	–	–
H_d	0.27	0.77	28.34	0.367	1.06	51.60	1.36	2.52	20.06
$Isel_d$	0.31	0.52	5.31	0.34	0.97	94.71	–	–	–
$Rish_d$	0.31	0.476	7.14	0.32	0.815	92.14	–	–	–

Table 6. Swelling index and rheological properties of montmorillonite

N	S	O	O	S	D	D
		600 rpm(CPs)	300 rpm(CPs)		600 rpm(CPs)	300 rpm(CPs)
1%	21	5	2	54	13	7
2%	23	9	7	75	22	14
3%	42	12	9	98	30	16
4%	55	13	9	110	38	20
5%	45	13	9	118	43	26

N = Na_2CO_3; S = swelling index; O = original; D = deferrated.

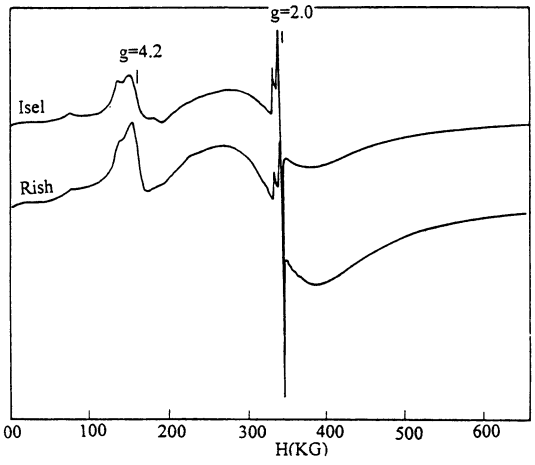

Fig. 7. ESR of original kaolinite samples (Isel and Rish). The symbols are the same as in Fig. 2.

Relationship between Fe and the parameters for kaolinite samples

All the parameters used for the characterization of different kaolinites were generally interconnected and also the iron content of kaolinite was an important common factor in many correlations. With the present kaolinite samples, the relationships between the crystallinite index (CI) measured following Hinkley (1963) and the total iron content as well as structural-Fe are shown in Table 3, which confirms a trend reported in literature: an increase in the total iron content is associated with an exponential decrease in the crystallinity of kaolinite. However, the crystallinity index of (H) sample is influenced by Fe_2/Fe_3 ratio (see Mössbauer results). This result may be attributed to the disturbance caused to the surface of (H) kaolinite by the larger radius of Fe^{2+} (78 pm) as compared to Fe^{3+} (64.5 pm) and Al^{3+} (53.5 pm). Fired color is the most significant property in the classification of the kaolin for commercial uses. The brightness of original kaolinite samples was measured (Table 7). Marked differences in brightness values for these samples may be related to the

nature and amounts of free Fe-oxide and oxyhydroxide associated with the kaolinite samples. Meanwhile, the colors of kaolinite samples after firing in an oxidizing condition (1250℃) were light-yellow to black-red when passing from (H) sample (0.5% Fe) to (Rish) sample (5.98% Fe). The color developed after firing is dependent on the percentage of coloring oxides, namely hematite and goethite and the enclosed Fe (Fe^{2+}, Fe^{3+}) in the kaolinite lattice. These can be explained by the formation of hematite through thermal decomposition of kaolinite mineral, with increasing temperature (1450℃) hematite is partially converted to magnetite and consequently the red color changed to black-red color, especially in Rish sample. However, the deferrated samples' brightness was significantly improved owing to removal of staining iron. Moreover, Fe plays an important role in the vitrification of kaolinite minerals. Thus, in the presence of large quantities (>5%) of iron (e.g. Rish sample), there may be little development in distinct high-temperature crystalline phases if compared with Isel sample. The presence of such flux in the Rish clay material may cause vitrification and fusion at temperatures as low as 900℃ and consequently enable closing open pores with the development of liquid phase. On cooling, the SiO_2-rich phase is solidified to a glass bond, leading to an increase in strength and shrinkage of the product at lower temperatures while porosity moves in the opposite direction (El-Khole et al., 1994). Therefore, the high content of iron in Rish kaolinite deposit restricts its application as fine ceramics. However, it is a suitable raw material for the production of engineering brick, which is commonly used in lining sewage pipes and tunnels as well as in industrial chimneys and in contact with acid. Meanwhile, K, H and Isel kaolinite deposits are suitable in sanitary as the glaze is usually colored and opaque.

Table 7. Brightness of kaolinite samples

Sample No.	Brightness		
	Original	Deferrated	Fired at 1250℃
K	61	81	72
H	65	81	73
Isel	34	73	45
Rish	25	74	19.5

References

Bahranowski, E., L. Serwicka Stoch, and P. Strycharski, 1993, On the possibility of removal of non-structural iron from kaolinite-group minerals: Clays and clay minerals, v.28, p.379－391.

Blakmore, A., 1973, Aggregation of clay by the products of iron (Ⅲ) hydrolysis: Aust. J. Soil Res., v.11, p.75－82.

Buatier, M., K. Ouyang, and J. Sanchez, 1993, Iron in hydrothermal clays from the Galapagos spreading center mounds: consequences for the clay transition mechanism: Clay Minerals, v.28, p.641－655.

Childs, C., B. Goodman, and G. Churhman, 1987, Application of Mössbauer spectroscopy to the study of oxides in some red and yellow/brown soil samples from New Zealand: Devel. in sedi No.27, Inter. Clay Conf.

Coey, J., 1980, Clay minerals and their transformation studies with nuclear techniques: Energy Rev., v.18, p.73－123.

El-Kholi, M., A. Meshrif, S. Abu Laban, and M. Serry, 1994, Application of Aswan clays for the production of acid resistant engineering bricks: Min. Soc. of Egypt, Int. Symp. On Ind. Appli. of Clay, Egypt.

Farmer, V., J. Russell, J. Ahlrichs, and B. Velde, 1967, Bull. Gr. Argiles, v.19, p.5.

Goodman, B., J. Russell, H. Fraser, and F. Woodhams, 1978, A Mössbauer and IR spectroscopic study of the structure of montmorillonite: Clays and Clay Minerals, v.24, p.53－59.

Grman, D., M. Pisár, and V. Novák, 1973, Silikáty, v.17, p.55.

Heller-Kallai, C. and L. Rozenson, 1981, The use of Mössbauer spectroscopy of iron in clay mineralogy: Phys. Chem. Minerals, v.7, p.223－238.

Heller, L., V. Farmer, R. Mackenzie, B. Mitchell, and H. Taylor, 1962, Clay Minerals: Bull., v.5, p.56.

Hinckley, D., 1963, Variability in crystallinity values among the kaolin deposits of the coastal plain of Georgia and South Carolina: Clays and Clay Minerals, II, p.229－235.

Kinniburgh, D., J. Syers, and M. Jakson, 1975, Specific adsorption of trace amounts of calcium and strontium by hydrous oxides of iron and aluminum: Soil Soc. Am. J., v.39, p.464－470.

McBride, M., T. Pinnavaia, and M. Mortland, 1975, Perturbation of structural Fe^{3+} in smectites by exchange ions: Clays and Clay Minerals, v.23, p.103－108.

Mehra, O. and M. Jackson, 1960, Iron oxide removal from soils and clays by dithonite-citrate system buffered with sodium bicarbonate: Clays and Clay Minerals, v.7, p.317－327.

Mestdagh, M., L. Vielvoye, and A. Herbillon, 1980, Iron in kaolinite, Ⅱ. the relationship between crystallinity and iron content: Clay Minerals, v.15, p.1－13.

Mendelovici, E., S. Yariv, and R. Villalba, 1979, Iron-bearing kaolinite in Venezuelan laterites: Clays and Clay Minerals, p.323－331.

Michalet, B., Guillet, and B. Souchier, 1993, Hematite identification in pseudo-particles of Moroccan Rubified soils: Clay Minerals, v.28, p.233－242.

Muard, E. and U. Wagner, 1994, The Mössbauer spectra of illite and their firing products: Clay Minerals, v.29, p.1－10.

Pedro, G., A. Chauvel, and J. Melfi, 1976, Recherches sur la constitution et la genese des Terra Rossa Estructurada du Bresil: Ann Argon, v.27, p.265－294.

Robet, M., J. Berrier, G. Veneau, and M. Vincente, 1981, Action of amorphous compounds on clay particle associations: Proc. 7th Int. Clay Conf., Bologna-Pavia, p.411－423.

Rozenson, I. And L. Heller-Kallai, 1977, Mössbauer spectra of dioctahedral smectite: Clays and Clay Minerals, v.25, p.94－101.

Shaikum, N. and R. Carr, 1987, Electron spin resonance studies of halloysites: Clays and Clay Minerals, v.22, p.287－296.

Stuki, J. and C. Roth, 1976, Clays and Clay Minerals: v.24, p.293.